Frequency Adaptive Selective Harmonic Control for Grid-Connected Inverters

Yang, Yongheng; Zhou, Keliang; Wang, Huai; Blaabjerg, Frede; Wang, Danwei; Zhang, Bin

Published in:
IEEE Transactions on Power Electronics

DOI (link to publication from Publisher):
10.1109/TPEL.2014.2344049

Publication date:
2015

Document Version
Early version, also known as pre-print

Frequency Adaptive Selective Harmonic Control for Grid-Connected Inverters

Yongheng Yang, *Student Member, IEEE,* Keliang Zhou, *Senior Member, IEEE,*
Huai Wang, *Member, IEEE,* Frede Blaabjerg, *Fellow, IEEE,*
Danwei Wang, *Senior Member, IEEE* and Bin Zhang, *Senior Member, IEEE*

***Abstract*—In this paper, a Frequency Adaptive Selective Harmonic Control (FA-SHC) scheme is proposed. The FA-SHC method is developed from a hybrid SHC scheme based on the internal model principle, which can be designed for grid-connected inverters to optimally mitigate feed-in current harmonics. The hybrid SHC scheme consists of multiple parallel recursive ($nk\pm m$)-order (k = 0, 1, 2, . . ., and $m \leq n/2$) harmonic control modules with independent control gains, which can be optimally weighted in accordance with the harmonic distribution. The hybrid SHC thus offers an optimal trade-off among cost, complexity and also performance in terms of high accuracy, fast response, easy implementation, and compatible design. The analysis and synthesis of the hybrid SHC are addressed. More important, in order to deal with the harmonics in the presence of grid frequency variations, the hybrid SHC is transformed into the FA-SHC, being the proposed fractional order controller, when it is implemented with a fixed sampling rate. The FA-SHC is implemented by substituting the fractional order elements with the Lagrange polynomial based interpolation filters. The proposed FA-SHC scheme provides fast on-line computation and frequency adaptability to compensate harmonics in grid-connected applications, where the grid frequency is usually varying within a certain range (e.g., 50±0.5 Hz). Experimental tests have demonstrated the effectiveness of the proposed FA-SHC scheme in terms of accurate frequency adaptability and also fast transient response.**

***Index Terms*—Harmonics, frequency variation, repetitive control, resonant control, harmonic control, grid-connected inverters**

I. Introduction

SEVERE Power Quality (PQ) problems have been brought by an increase of renewable energy systems, e.g. Photo-Voltaic (PV) systems and wind turbine systems, as well as the power electronics interfaced loads [1]–[4]. The energy conversion is typically performed by power electronics converters, which will produce harmonics during operation [5], [6]. Since the emitted harmonic to the grid may bring additional power losses, trigger resonances, cause device malfunction, and even induce system instability, grid-interconnection rules [7], [8] have been published as a guidance for the design, control, and operation of grid-connected converters, e.g. PV inverters. In order to meet PQ requirements, it calls for optimal harmonic control strategies to compensate these periodic harmonic contents with high control accuracy, while maintaining fast transient response, guaranteeing robustness, and also being feasible for easy implementation [3], [9]–[11].

Regarding control accuracy, by the Internal Model Principle (IMP) [12], zero error tracking of any periodic signal (e.g. grid current) in steady-state can be achieved, as long as a generator of the reference is included in a stable closed control loop. Many IMP-based controllers have been developed for grid-connected inverters, e.g. Repetitive Controller (RC) [3], [13]–[19], ReSonant Controller (RSC) [9], [20], [21], and hybrid controllers [3], [22]. There are also other control strategies which can selectively compensate the harmonic distortion by modifying the modulation schemes, as presented in [23]–[26]. The above IMP-based controllers offer relative accurate control of periodic signals as internal models of interested harmonics have been included into the control loop. However, optimal mitigation of the harmonics by those controllers is difficult to achieve even considering the fact of unequal harmonic distributions [4], [17], [27]–[29]. For example, the conventional recursive RC, which includes the internal models of all harmonics, has an identical control gain, and thus fails to optimally suppress selective harmonics and the transient response is also slow. Taking the harmonic distribution into account, multiple parallel resonant controllers and the discrete Fourier transform based RC consisting of the internal models of selected harmonics with independent control gains, can render quite fast transient response at the cost of parallel computation burden and design complexity.

To address this issue, an IMP based Selective Harmonic Control (SHC) named "($nk \pm m$)-order harmonic RC", which only includes internal models of $nk\pm m$ ($m \leq n/2$ and n is the pulse number) order harmonics, has been introduced in [13], [17] and [30] to optimally mitigate the harmonics. Compared to the conventional RC, the ($nk \pm m$)-order harmonic RC features with:

1) up to $n/2$ times faster convergence rate at selected ($nk\pm m$)-order harmonics;
2) less memory elements for the computation and easy for implementation;

Manuscript received May 7, 2014; revised July 7, 2014; accepted July 26, 2014. Recommended for publication by Associate Editor xxx.

Y. Yang, H. Wang, and F. Blaabjerg are with the Department of Energy Technology, Aalborg University, Aalborg 9220, Denmark (e-mail: yoy@et.aau.dk;hwa@et.aau.dk;fbl@et.aau.dk). K. Zhou (*Corresponding Author*) is with the School of Engineering, University of Glasgow, Glasgow G12 8QQ, UK (e-mail: eklzhou@ieee.org). D. Wang is with the School of Electrical and Electronic Engineering, Nanyang Technological University, Singapore 639798 (e-mail: edwwang@ntu.edu.sg). B. Zhang is with the Department of Electrical Engineering, University of South Carolina, Columbia SC 29208, USA (e-mail: zhangbin@cec.sc.edu).

Color versions of one or more of the figures in this paper are available online at http://ieeexplore.ieee.org

Digital Object Identifier 10.1109/TPEL.2014.xxxxxxx

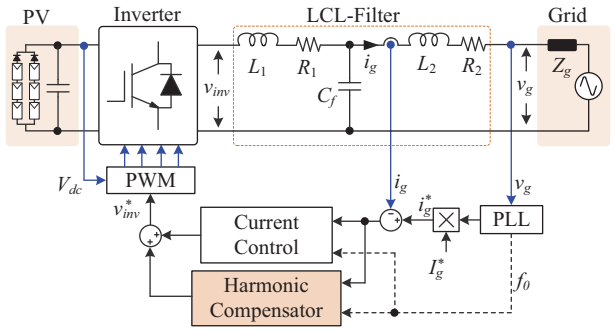

Fig. 1. Typical current control structure of a single-phase grid-connected PV inverter with an *LCL*-filter.

3) compatible design in contrast to the conventional RC.

In fact, the $(nk \pm m)$-order harmonic RC control scheme provides a framework for housing various SHC schemes, e.g. the conventional RC where all the harmonics are compensated, the odd harmonic RC [28], [29] and "$6k \pm 1$" RC for three-phase systems [20], [27], [31]. Moreover, another compatible $(nk \pm m)$-order harmonic RC named "general parallel structure RC" has been proposed lately [17]. Since it includes multiple parallel $(nk \pm m)$-order harmonic RC with independent control gains, a good trade-off among control accuracy, transient response, and implementation complexity can be achieved. The dual mode RC [18] is actually a special case of the "general parallel structure RC". In this paper, based on the "$(nk \pm m)$-order harmonic RC", a hybrid SHC has been introduced and developed, which allows an optimal parameter tuning for the $(nk \pm m)$-order harmonic RC controlled grid-connected systems in contrast with the "general parallel structure RC".

However, all above IMP-based harmonic controllers, especially the $(nk \pm m)$-order harmonic RC based schemes, are sensitive to frequency variations, and also require a specific fixed sampling rate dependent on the fundamental frequency when implemented [32], [33]. For example, for a 60 Hz system, the sampling frequency has to be multiple times of 60 Hz (e.g. 12 kHz). Additionally, the grid frequency f_0 is practically not a constant but within a certain range (e.g. 59 Hz$\sim$ 61Hz) [34], [35]. Consequently, the number of samples per period $N = f_s/f_0$ for fundamental frequency harmonics and/or the period N/n for $(nk \pm m)$-order harmonics are fractional (i.e. non-integer) in the case of a fixed sampling rate f_s. However, the above controllers can accurately compensate any harmonics only with a known integer N in a digital control system, but in the case of varying the grid frequency, the tracking accuracy will be degraded. So variable grid frequencies can contribute to significant performance degradation of the harmonic mitigation for grid-connected systems and thus frequency adaptive controllers have become favorable for those applications [2], [36]–[39].

Using variable sampling rate is a possibility to always ensure an integer period N in the case of grid frequency variations, and thus enable the above IMP-based harmonic controllers to eliminate selected harmonics completely [31], [37], [40], [41]. However, doing so will increase the implementation complexity of the digital control system, e.g. online

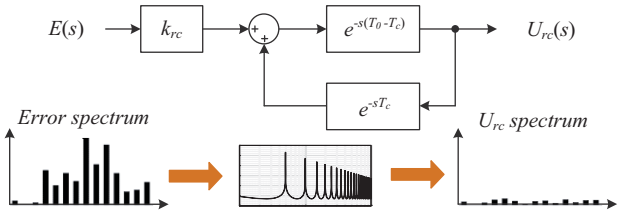

Fig. 2. Conventional repetitive controller $G_{rc}(s) = U_{rc}(s)/E(s)$.

controller redesign. In the light of these issues, a fractional order RC strategy with a fixed sampling rate is proposed to accurately compensate power harmonics of variable frequencies [32], [42]. The delay z^{-F} with a fractional order number F can be well approximated by a *Lagrange* interpolation based filter [43], [44]. The fractional delay filter applied in the conventional RC scheme only requires a few multiplications and additions for coefficient update, and thus it is suitable for fast online tuning of the fractional order controller. Preliminary results demonstrate the validity of the fractional order RC strategy in these literature. However, a frequency adaptive $(nk \pm m)$-order harmonic RC with a fixed sampling rate is still open.

In view of this, a Frequency Adaptive hybrid SHC (FA-SHC) scheme is proposed in this paper. The proposed FA-SHC is based on the integer-period "$(nk \pm m)$-order harmonic RC". Compared with the conventional RC and the $(nk \pm m)$-order harmonic RC, the control gains of the proposed FA-SHC can be optimally weighted to achieve desirable harmonic mitigation in grid-connected inverter systems. Compatible design criteria of the hybrid SHC scheme are firstly given in § II to facilitate the synthesis of this control method. Then, to precisely compensate variable frequency harmonics, the hybrid SHC with a fixed sampling rate is transformed from an integer-order controller into a general fractional order one, being the proposed FA-SHC scheme, and it is introduced in § III. Experimental verifications of a single-phase grid-connected inverter system are provided in § IV to verify the effectiveness of the proposed FA-SHC.

II. Selective Harmonic Control

A. Conventional Repetitive Control

The Conventional RC (CRC) has been an effective harmonic controller for periodic signals, e.g. grid currents. Generally, the CRC is adopted to enhance the control performance in terms of harmonic compensations, as it is exemplified in Fig. 1, where typically the Total Harmonic Distortion (THD) of the injected current i_g should be lower than 5 % [7], [8]. To accomplish a lower current THD, the CRC represented in Fig. 2 can be employed as the harmonic compensator shown in Fig. 1. According to Fig. 2, the CRC can be expressed in the continuous-time domain as,

$$G_{rc}(s) = \frac{U_{rc}(s)}{E(s)} = \frac{k_{rc} \cdot e^{-sT_0}}{1 - e^{-sT_0}} \cdot e^{-sT_c} \qquad (1)$$

where k_{rc} is the control gain, $T_0 = 1/f_0 = 2\pi/\omega_0$ is the fundamental period of the signals with ω_0 being the

fundamental angular frequency, and T_c is the phase lead compensation time.

The CRC controller shown in (1) is recursive, and thus consumes a little computation effort when it is implemented. The CRC RC controller, $G_{rc}(s)$, can further be expanded as [3], [17],

$$G_{rc}(s) = k_{rc}\left[-\frac{1}{2} + \frac{1}{sT_0} + \frac{1}{T_0}\sum_{h=1}^{\infty}\frac{s}{s^2+(h\omega_0)^2}\right] \quad (2)$$

which indicates that the CRC is equivalent to a combination of a proportional controller (i.e., $-k_{rc}/2$), an integrator (i.e., $k_{rc}/(sT_0)$), and multiple parallel RSCs at all harmonic frequencies (i.e., the internal models of DC and all harmonic signals). According to IMP, the RSC components approach infinity at harmonic frequencies $h\omega_0$ (including DC signal), and thus the CRC shown in (1) is able to compensate all harmonic distortions as shown in Fig. 2. It is worth to point out that, a large control gain for an RSC contributes to a fast transient response at the corresponding harmonic frequency [1], [11]. Since the control gains for all RSC controllers of the CRC are identical, i.e. k_{rc}/T_0 in (2), it is impossible for the CRC to optimize its transient response by individually tuning the control gain at each harmonic frequency. Consequently, the CRC presents an accurate but slow selective harmonic compensation performance as discussed in [17], [18], [28].

B. Selective Harmonic Control

Multiple parallel RSCs $G_{res}(s)$ acts at selected harmonic frequencies, and it can achieve a fast transient response as the control gains are independent. This controller is an intuitive way to compensate selective harmonics as follows [9], [10], [41]:

$$G_{res}(s) = \sum_{h=1,2,\ldots} k_h\frac{s\cos(\omega_h\tau_h) - \omega_h\sin(\omega_h\tau_h)}{s^2+\omega_h^2} \quad (3)$$

in which h is the harmonic order with ω_h and k_h being the corresponding angular frequency and control gain, τ_h is the phase lead compensation time at ω_h. Compared to the CRC shown in (1), the multiple RSCs, $G_{res}(s)$, have independent control gains k_h and phase lead compensation time τ_h to optimize its transient response at selected harmonics, and thus can achieve a fast response if k_h is large enough. However, to achieve a satisfactory accuracy, high-order harmonics have to be compensated, leading to much tuning difficulty and many multiplications and summations.

Since the harmonics are not distributed equally as shown in Fig. 2, compensating selected $(nk \pm m)$-order harmonic frequencies is feasible. Thus, a recursive SHC module (i.e., $(nk\pm m)$-order harmonic RC), which only includes the internal models of all $(nk \pm m)$-order harmonics, can be adopted as follows [13], [17], [45]:

$$\begin{aligned} G_{nm}(s) &= \frac{k_m}{2}\left[\frac{e^{-s\frac{T_0}{n}+j\frac{2\pi m}{n}}}{1-e^{-s\frac{T_0}{n}+j\frac{2\pi m}{n}}} + \frac{e^{-s\frac{T_0}{n}-j\frac{2\pi m}{n}}}{1-e^{-s\frac{T_0}{n}-j\frac{2\pi m}{n}}}\right] \\ &= k_m\frac{\cos(\frac{2\pi m}{n})e^{s\frac{T_0}{n}}-1}{e^{2s\frac{T_0}{n}}-2\cos(\frac{2\pi m}{n})e^{s\frac{T_0}{n}}+1}e^{sT_c} \end{aligned} \quad (4)$$

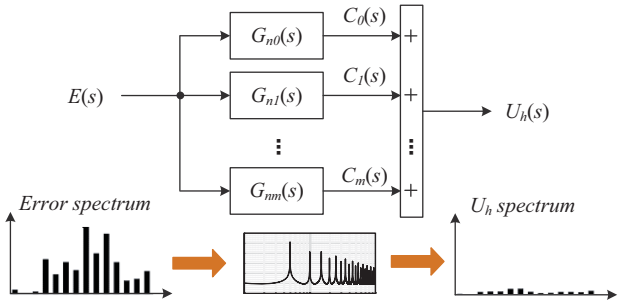

Fig. 3. Generic selective harmonic controller, $G_{SHC}(s) = U_h(s)/E(s)$.

where n, m are integers with $0 \le m \le n/2$, k_m is the control gain, and T_0, T_c have been defined previously. Additionally,

$$\begin{aligned} \frac{e^{-2\pi\left(\frac{s}{n\omega_0}\pm\frac{jm}{n}\right)}}{1-e^{-2\pi\left(\frac{s}{n\omega_0}\pm\frac{jm}{n}\right)}} &= -\frac{1}{2} + \frac{n}{T_0}\frac{1}{(s\pm jm\omega_0)} \\ &\quad + \frac{n}{T_0}\sum_{k=1}^{+\infty}\frac{2(s\pm jm\omega_0)}{(s\pm jm\omega_0)^2+(nk\omega_0)^2} \end{aligned} \quad (5)$$

in which $k = 0, 1, 2, \ldots$, and $m = 0, 1, 2, \ldots, n/2$. It is observed from (5) that the SHC module $G_{nm}(s)$ is equivalent to a parallel combination of RSCs at $(nk\pm m)$-order harmonic frequencies. According to IMP, the SHC module can achieve zero tracking error at selected $(nk \pm m)$-order harmonics without too much parallel computation burden (less multiplications and summations) in contrast to multiple RSCs ($G_{res}(s)$). In respect to the transient response, since the convergence rate of any RSC is proportional to its control gain, the error convergence rate at $(nk \pm m)$-order harmonic frequencies of the SHC module shown in (4) can be $n/2$ times faster if $k_m = k_{rc}$.

In practical applications, a modified SHC module $G_{nm}(s)$ is employed as (6), where $G_f(s) = e^{sT_c}$ is a phase-lead compensation filter to stabilize the overall closed-loop system, and a low-pass filter $Q(s)$ is employed to make a good tradeoff between the tracking accuracy and the system robustness. The SHC module given by (4) and (6) provides a recursive IMP-based controller, which is tailored for $(nk\pm m)$-order harmonic frequencies. For instance, let n=1 and m=0, it becomes a CRC, and let n=4 and m=1, it becomes an odd harmonic RC [28], [29]. It is generally named as "$(nk \pm m)$-order harmonic RC" in [30].

To provide a more convenient SHC control solution, a generic hybrid SHC scheme is developed to further improve the power harmonic compensation as follows,

$$G_{SHC}(s) = \sum_{m\in N_m} G_{nm}(s) \quad (7)$$

where m and N_m represent $(nk \pm m)$-order harmonics and the set of selected harmonic frequencies ($N_m \le n/2$), respectively. Fig. 3 shows the hybrid SHC control scheme, which can contribute to an optimal tradeoff between control accuracy and transient response when considering the harmonics distribution. The parallel SHC modules can be flexibly designed to optimize its control accuracy, and individual control gains k_m can be flexibly weighted to optimize its

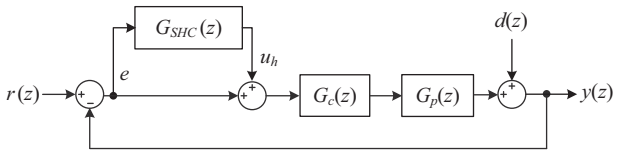

Fig. 4. Digital plug-in hybrid selective harmonic control system.

transient response based on the harmonic distribution. When the control gains (k_m) are identical, the hybrid SHC shown in (7) is equivalent to the CRC given by (1) with the control gain being $k_{rc} = 0.5k_m/n$ [14], [17]. The dual mode structure RC presented in [18] is a special case of the hybrid SHC with n = 4 and m = 0, 1, 2.

C. Design Criteria of Selective Harmonic Control

Since nowadays most control systems are implemented in the digital signal processors, the following are discussed in z-domain. Fig. 4 shows a typical closed-loop digital control system with the plug-in hybrid SHC controller, where $G_p(z)$ is the transfer function of the plant, $G_c(z)$ is a feedback controller, $G_{SHC}(z)$ is the corresponding hybrid SHC given by (7) in z-domain, $r(z)$ is the reference sinusoidal signal (e.g., i_g^* in Fig. 1), $y(z)$ is the output, $e(z) = r(z) - y(z)$ is the tracking error and the input of $G_{SHC}(z)$, and $d(z)$ is the disturbance.

Moreover, the output $y(z)$ of the plug-in hybrid SHC controlled system can be expressed as,

$$y(z) = \frac{[1 + G_{SHC}(z)]H(z)}{1 + G_{SHC}(z)H(z)} r(z) + \frac{[1 + G_c(z)G_p(z)]^{-1}}{1 + G_{SHC}(z)H(z)} d(z) \tag{8}$$

where $H(z)$ is the transfer function of a conventional closed-loop feedback control system without plugging in the hybrid SHC controller $G_{SHC}(z)$, and they can be expressed as,

$$\begin{aligned} G_{SHC}(z) &= \sum_{m \in N_m} G_{nm}(z) \\ &= \sum_{m \in N_m} \frac{k_m z^c \left[\cos(\frac{2\pi m}{n}) z^{\frac{N}{n}} Q(z) - Q^2(z)\right]}{z^{\frac{2N}{n}} - 2\cos(\frac{2\pi m}{n}) z^{\frac{N}{n}} Q(z) + Q^2(z)} \end{aligned} \tag{9}$$

$$H(z) = \frac{G_c(z)G_p(z)}{1 + G_c(z)G_p(z)} \tag{10}$$

in which N and k_m have been defined previously, $G_f(z) = z^c$ is the phase-lead compensation filter $G_f(s)$ in z-domain, and $Q(z)$ is a low-pass filter with $|Q(e^{j\omega})| \leq 1$. The low-pass filter $Q(z)$ is employed to make a good tradeoff between the tracking accuracy and the system robustness, since it removes minor but unexpected high frequency disturbances with $|Q(e^{j\omega})| \to 1$ at low frequencies and $|Q(e^{j\omega})| \to 0$ at high frequencies, e.g. $Q(z) = \alpha_1 z + \alpha_0 + \alpha_1 z^{-1}$ with $2\alpha_1 + \alpha_0 = 1$, $\alpha_0 > 0$ and $\alpha_1 > 0$ [14], [29].

Without loss of generality, $H(z)$ can be described by,

$$H(z) = \frac{B(z)}{A(z)} = \frac{z^{-d} B^+(z) B^-(z)}{A(z)} \tag{11}$$

where d represents the known delay steps with $d \in [0, N/n]$, all the roots of $A(z)$ are inside the unit circle, $B(z)$ and $(z^{N/n} - e^{j2\pi m/n}) \cdot (z^{N/n} - e^{-j2\pi m/n})$ are co-prime, and $B^+(z)$, $B^-(z)$ are the cancellable and un-cancellable parts of $B(z)$, respectively. $B^-(z)$ comprises roots on or outside the unit circle and undesirable roots in the unit circle, and $B^+(z)$ comprises roots of $B(z)$, which are not in $B^-(z)$.

Considering the feedback control system $H(z)$, a modified phase lead compensator $G_f(z)$ is employed as,

$$G_f(z) = \frac{z^c A(z) B^-(z^{-1})}{B^+(z) b} \tag{12}$$

where the phase lead step $c = d$ and $b \geq \max(|B^-(e^{j\omega})|^2)$. Since the SHC module will generate periodical signals of (N/n)-step delay $z^{-\frac{N}{n}}$ ($n \ll N$ and $\frac{N}{n} \geq d$), $G_f(z)$ with non-causal component z^d can be physically implemented.

From (11) and (12), $G_f(z)H(z) = |B^-(e^{j\omega})|^2/b$ is constant, i.e. the phase lag of $H(z)$ is perfectly compensated by $G_f(z)$. This will significantly simplify the synthesis of the plug-in hybrid SHC system. Based on this, the hybrid SHC controlled system with $Q(z)$=1 in Fig. 4 will be asymptotically stable if the following are satisfied [13], [17], [30]:

1) $H(z)$ is asymptotically stable;
2) Control gains k_m (≥ 0) meet the following constraint:

$$0 < \sum_{m \in N_m} k_m < 2. \tag{13}$$

Obviously, the above stability criteria for the hybrid SHC scheme can be derived from those for parallel structure digital RC control systems [30], [45], and are compatible to those for other digital RC control solutions [17]–[19], [28]–[30], [46]. It should be noted that the developed hybrid SHC scheme offers grid-connected power converters an optimal IMP-based control solution to harmonic mitigation in terms of high accuracy, fast transient response, cost-effective and easy real-time implementation, and compatible design rules. The synthesis method for this hybrid SHC scheme has been given by (8)-(13).

III. Frequency Adaptive Selective Harmonic Control

Either the hybrid SHC or the CRC is sensitive to harmonic frequency variations, e.g. grid frequency fluctuation in grid-connected inverter systems. Moreover, even in a stable frequency system, the sampling frequency must be selected to

$$G_{nm}(s) = \frac{k_m G_f(s)}{2} \left[\frac{e^{-s\frac{T_0}{n} + j\frac{2\pi m}{n}} Q(s)}{1 - e^{-s\frac{T_0}{n} + j\frac{2\pi m}{n}} Q(s)} + \frac{e^{-s\frac{T_0}{n} - j\frac{2\pi m}{n}} Q(s)}{1 - e^{-s\frac{T_0}{n} - j\frac{2\pi m}{n}} Q(s)} \right] = \frac{k_m G_f(s) \left[\cos(\frac{2\pi m}{n}) e^{s\frac{T_0}{n}} Q(s) - Q^2(s)\right]}{e^{2s\frac{T_0}{n}} - 2\cos(\frac{2\pi m}{n}) e^{s\frac{T_0}{n}} Q(s) + Q^2(s)} \tag{6}$$

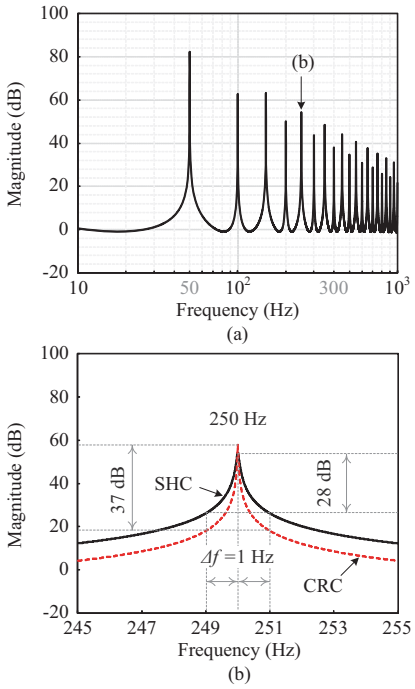

Fig. 5. Magnitude response of a hybrid selective harmonic controller (SHC): (a) within a frequency range of 10 Hz to 1 kHz and (b) illustration of frequency sensitivity at the 5th-order harmonic.

ensure an integer period $N = f_s/f_0$ for the CRC and an integer period $p = N/n$ for the hybrid SHC control scheme. The harmonic compensation accuracy will be deteriorated if an integer period CRC of a period $\lfloor N \rfloor$ or hybrid SHC of a period $\lfloor p \rfloor$ is adopted to compensate fractional period harmonics. It is therefore necessary to develop frequency adaptive controller for grid-connected inverters to assure high tracking accuracy in the presence of variable grid frequencies.

Assuming that $z^{-p} = z^{-(P+F)}$ with the superscript $P = \lfloor p \rfloor$ being the integer part of p, the superscript F being the fractional part of p with $0 \le F < 1$, and $G_f(z) = z^c$, the hybrid SHC shown in (9) can then be written as,

$$G_{FA-SHC}(s) = \sum_{m\in N_m} \frac{k_m z^c \left[\cos\left(\frac{2\pi m}{n}\right) z^p Q(z) - Q^2(z)\right]}{z^{2p} - 2\cos\left(\frac{2\pi m}{n}\right) z^p Q(z) + Q^2(z)}$$
$$= \sum_{m\in N_m} \frac{k_m z^c \left[\cos\left(\frac{2\pi m}{n}\right) z^{P+F} Q(z) - Q^2(z)\right]}{z^{2(P+F)} - 2\cos\left(\frac{2\pi m}{n}\right) z^{P+F} Q(z) + Q^2(z)} \quad (14)$$

It can be seen from (9) and (14) that, the hybrid SHC scheme is sensitive to frequency variations. If the fractional part F of the period p is omitted in (14), i.e. $F = 0$ and $z^{-p} = z^{-P}$, the infinity gains of the integer order $G_{SHC}(z)$ will be shifted away from the selected harmonic frequencies of interest, and may lead to a significant degradation of the control accuracy consequently.

For instance, the magnitude response of a hybrid SHC for periodic signals of fundamental frequency $f_0 = 50$ Hz is shown in Fig. 5(a), where $N = 200$ in case of the sampling frequency of 10 kHz, $\sum k_m = k_{rc} = 1.8$, $Q(z) = 0.05z + 0.9 + 0.05z^{-1}$ and $G_f(z) = z$. Fig. 5(b) shows the magnitude response of the hybrid SHC and CRC at the neighborhood of the 5th-order harmonic, which demonstrates the frequency sensitivity of both the hybrid SHC and CRC schemes. It can be observed from Fig. 5(b) that, if the fundamental frequency changes from 50 Hz to 50±0.2 Hz, the corresponding magnitude at the 5th-order harmonic frequency will drop from 55.07 dB at 250 Hz to 18.09 dB at 250±1 Hz for the CRC, whilst from 54.3 dB to 26.2 dB for the hybrid SHC. This demonstrates that an integer-order hybrid SHC or CRC cannot accurately compensate fractional-order harmonics. It can also be seen from Fig. 5(b) that the CRC is more sensitive to frequency variation than the hybrid SHC.

In view of this issue, a frequency adaptive hybrid SHC scheme is proposed in the following. On the basis of the Fractional Delay (FD) filter design methods [33], [42], [43], the factional-order part z^{-F} of z^{-p} due to a fixed sampling rate or frequency variations can be well approximated by a *Lagrange* interpolation polynomial Finite-Impulse-Response (FIR) filter. The approximation can be expressed as [32], [43],

$$z^{-F} \approx \sum_{l=0}^{N_D} D_l z^{-l} \quad (15)$$

and

$$D_l = \prod_{\substack{i=0 \\ i\neq l}}^{N_D} \frac{F-i}{l-i},\ l = 0,\ 1,\ 2,\ ...,\ N_D \quad (16)$$

where N_D is the FD length (order), and D_l is the *Lagrange* interpolation polynomial coefficient. If N_D= 1, the approximation shown in (15) will become a linear interpolation polynomial, i.e. $z^{-F} \approx (1-F) + Fz^{-1}$, while a cubic interpolation if N_D= 3.

It should be pointed out that, achieving fast on-line tuning of the fractional period and fast update of the coefficients plays an important role in the real-time control of high switching frequency converters (e.g., grid-connected inverters). The *Lagrange* interpolation discussed above only takes a small number of multiplications and summations to update its output as shown in (16). It is therefore one of the most efficient ways to design a FD filter to approximate a given fractional delay (e.g. z^{-F}). As a consequence, this method can be utilized for the FA-SHC scheme with improved tracking accuracy, limited loss of transient response, and increased little computation burden compared to the hybrid SHC.

As it can be seen from (15) and (16), the higher the filter order N_D is, the more accurate the approximation is. However, a higher order FD will consume more computation time. The magnitude responses of the *Lagrange* interpolation based FD filters of order N_D = 1 and N_D = 3 for fractional delay F from 0 to 0.9 are shown in Fig. 6. It is seen that the FD filter of order N_D= 3 presents a good approximation of z^{-F} at low frequencies with a bandwidth of 75% of the *Nyquist* frequency (i.e., $f_s/2$), while a bandwidth of 50% of the *Nyquist* frequency in case of N_D= 1. Since the harmonic frequencies beyond the range of the pass band of low-pass filter $Q(z)$ cannot be completely compensated by the universal hybrid SHC, the proposed low-pass FD filter whose bandwidth

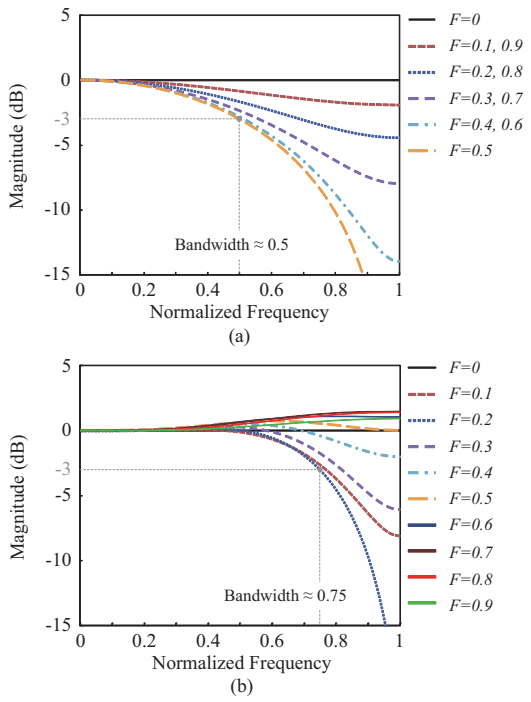

Fig. 6. Magnitude responses of fractional-order delay filters based on *Lagrange* interpolation: (a) $N_D = 1$ linear interpolation and (b) $N_D = 3$ cubic interpolation.

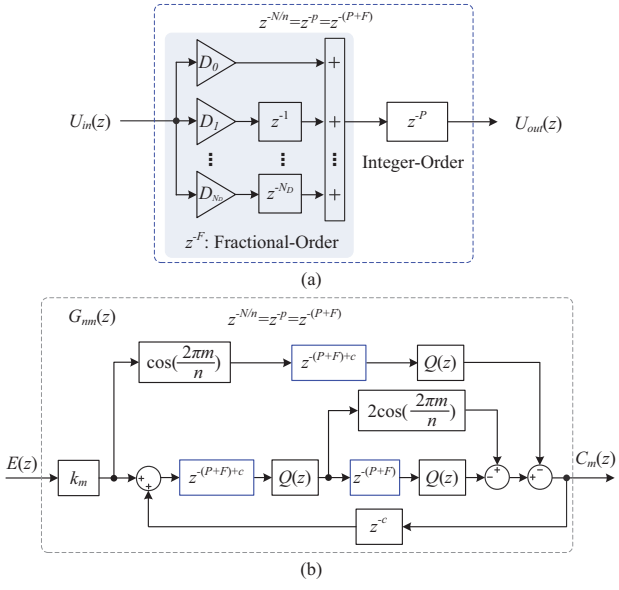

Fig. 7. Frequency adaptive selective harmonic control (FA-SHC): (a) implementation of the fractional-order delay $z^{-N/n}$ and (b) implementation of a FA-SHC module according to (14).

is larger than the bandwidth of $Q(z)$ could be used to replace the factional delay z^{-F} in practical applications.

In general, the *Lagrange* interpolation based FIR FD filter can not only easily be implemented in real-time applications, but it offers also high approximation accuracy in most cases. Substituting (15) and (16) into (14), a more convenient and effective hybrid SHC can be obtained with a fixed sampling frequency to compensate variable frequency harmonics in grid-connected applications. As it is shown in Fig. 7, the FA-SHC includes fractional-order SHC modules which enable the frequency adaptability of the hybrid SHC scheme. It should be pointed out that the aforementioned hybrid SHC of (7) is a special case of the proposed FA-SHC in case of F=0. The synthesis method for the proposed FA-SHC scheme is the same as that for the hybrid SHC scheme shown in Fig. 3, which has been given by (8)-(13) in details.

IV. Case Study: Experimental Verifications

A. System Modelling and Dead-Beat Control

In order to verify the effectiveness of the proposed FA-SHC control scheme, experimental tests have been performed on a single-phase grid-connected system referring to the control system shown in Fig. 1. For simplicity, the current controller is a Dead-Beat (DB) controller, which is illustrated in the following.

Referring to Fig. 1, the filter-capacitor C_f is used to eliminate high-order harmonics at the switching frequencies. Together with the grid-side inductor L_2, it can be considered as a "model mismatch" [47]. Therefore, the dynamic model of the single-phase grid-connected system shown in Fig. 1 can be simplified as,

$$L_1 \frac{di_g}{dt} + R_1 i_g = v_{inv} - v_g \tag{17}$$

where v_g is the grid voltage, i_g is the grid current, L_1 and R_1 are the inductance and resistance of the inductor, L_1, respectively. From (17), a DB current controller is obtained as,

$$v_{inv}^*(k) = \frac{1}{v_{dc}(k)} \left[v_g(k) + b_1 i_g^*(k) - (b_1 - b_2) i_g(k) \right] \tag{18}$$

in which $b_1 = L_1/T_s$, $b_2 = R_1$, k is the sampling number, and v_{dc} is the DC-link voltage. The DB controller in (18) will force the current to track the reference in one sampling period, i.e. $i_g(k+1) = i_g^*(k)$. However, due to model mismatches and system uncertainty, the control parameters, b_1 and b_2, can be adjusted to enhance the robustness of the controller [2], [47].

One control goal of the grid-connected inverter is to achieve a unity power factor, and thus a second-order generalized integrator based phase locked loop (PLL) system [1] is adopted to synchronize the grid current with the grid voltage. The other objective is to maintain a satisfactory harmonic-distorted sinusoidal feeding current (THD $<$ 5 %), and thus the proposed FA-SHC control schemes are plugged into the DB control system as the harmonic compensator shown in Fig. 1 to enhance the current tracking performance.

B. Experimental Results - Nominal Grid Frequency (50 Hz)

As seen from (1), (9), and (14), the discussed control schemes require a linear phase-lead filter $G_f(z) = z^c$ to approximately achieve a zero phase compensation [46]. The filter order $c = 3$ has been determined by experiments for the CRC, the hybrid SHC, and the proposed FA-SHC schemes. All the discussed controllers are implemented in a dSPACE 1103 system. It should be noted that those controllers can

TABLE I
SYSTEM PARAMETERS.

Parameter	Value
Nominal grid amplitude	$v_{gn} = 220\sqrt{2}$ V
Nominal grid frequency	$\omega_0 = 2\pi \times 50$ rad/s
Reference current amplitude	$I_g = 5$ A
Transformer leakage impedance	$L_g = 2$ mH, $R_g = 0.2\ \Omega$
	$L_1 = L_2 = 3.6$ mH
LCL-filter	$R_1 = R_2 = 0.04\ \Omega$
	$C_f = 2.35\ \mu$
Sampling and switching frequency	$f_s = f_{sw} = 10$ kHz
DC voltage	$V_{dc} = 400$ V
Repetitive controller gain	$k_{rc} = \sum_{m \in N_m} k_m = 1.8$

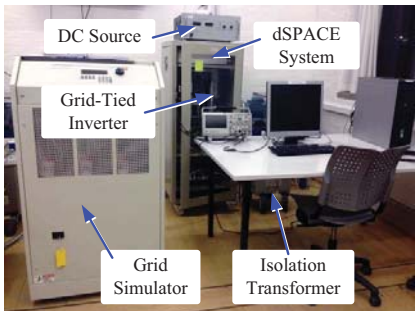

Fig. 8. Experimental setup of a single-phase grid-connected system.

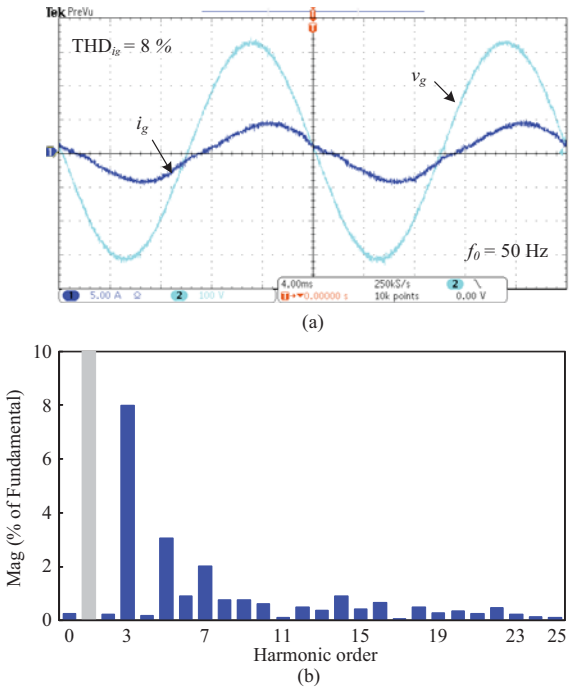

Fig. 9. Steady state performance of a DB controlled single-phase grid-connected system: (a) grid voltage v_g: [100 V/div] and grid current i_g: [5 A/div], time: [4 ms/div] and (b) harmonic spectrum of the grid current i_g.

also be implemented in a low-cost microcontroller, which has enough space to process the delays of those controllers (e.g., 0.02 s for the CRC) [48]. The test setup is shown in Fig. 8 and the system parameters are listed in Table I. A California Instruments AC Source is adopted as the simulated power grid. Instead of PV panels, a DC power source is utilized in the experiments. A commercial full-bridge PV inverter has been used as the power conversion stage, and thus it will dominantly introduce $(4k \pm 1)$-order harmonic currents, which are fed into the grid (grid simulator) through an LCL-filter and an isolation transformer as shown in Fig. 1.

In order to find the optimal control gains, k_m, for the plug-in hybrid SHC scheme and also the proposed FA-SHC scheme based on the harmonic distribution, the steady-state of the grid voltage v_g and grid current i_g only with DB control is presented in Fig. 9. The corresponding harmonic spectrum of the grid current i_g is shown in Fig. 9(b), where the harmonic order h=0, 2, 3, ... It can be obtained from Fig. 9 that, the ratio of all $4k$ (i.e., h=0, 4, 8, ...) order harmonics to the total harmonics is nearly 18 %, the ratio of all $4k \pm 1$ (i.e., h=3, 5, 7, ...) order harmonics to the total harmonics is nearly 62 %, and the ratio of all $4k \pm 2$ (i.e., h=2, 6, 10, ...) order harmonics to the total harmonics is nearly 20 %. Accordingly, the hybrid SHC controller can be employed as,

$$G_{SHC}(z) = \sum_{m \in N_m} G_{nm}(z) = G_{40}(z) + G_{41}(z) + G_{42}(z) \tag{19}$$

whose control gains k_0, k_1, k_2 for the SHC modules $G_{40}(z)$, $G_{41}(z)$, $G_{42}(z)$ satisfy $k_0 \le k_2 \le k_1$, and they are proportional to their ratios to the total harmonics. According to (13), the stability range of control gain k_{rc} for the CRC scheme is $0 < k_{rc} < 2$, and for the hybrid SHC or the proposed FA-SHC is $0 < k_0 + k_1 + k_2 < 2$. Since the error convergence rate is proportional to the control gain, the CRC control gain is chosen as $k_{rc} = k_0 + k_1 + k_2$ to facilitate the comparison between the CRC and the proposed FA-SHC (also the hybrid SHC), and the control gain k_m =1.8 is chosen for the $(4k \pm 1)$-order SHC controller. In the following experiments, the control gains for the hybrid SHC and the proposed FA-SHC schemes are optimally weighted according to the harmonic distribution as $k_0 = 0.2$, $k_1 = 1.4$, and $k_2 = 0.2$.

In order to evaluate the harmonic distribution of the injected current, i_g, a harmonic ratio $h_r(j)$ is defined as,

$$h_r(j) = \frac{\sum_{i=1}^{j} M_i}{\sum_{i=1}^{199} M_i} \times 100\% \tag{20}$$

in which M_i is the magnitude of the i-th order harmonic. Correspondingly, the harmonic ratio $h_r(j)$ for the current spectrum shown in Fig. 9(b) can be represented in Fig. 10(a), which indicates that over 83 % of the harmonics are of a certain range (0 $\sim$ 3.5 kHz). Consequently, if the cutoff frequency f_{cutoff} of low-pass filters (LPF) $Q(z)$ for the RC and $Q^2(z)$ for the hybrid SHC or the proposed FA-SHC are chosen as $f_{\text{cutoff}} > 3.5$ kHz, most of the harmonics will be removed by the CRC or the FA-SHC (also the hybrid SHC). As it is shown in Fig. 10(b), the cutoff frequencies of the designed $Q(z) = 0.1z + 0.8 + 0.1z^{-1}$ and $Q^2(z) = (0.05z + 0.9 + 0.05z^{-1})^2$ are 3.3 kHz and 3.5 kHz, respectively, and thus approximately meet the bandwidth requirement.

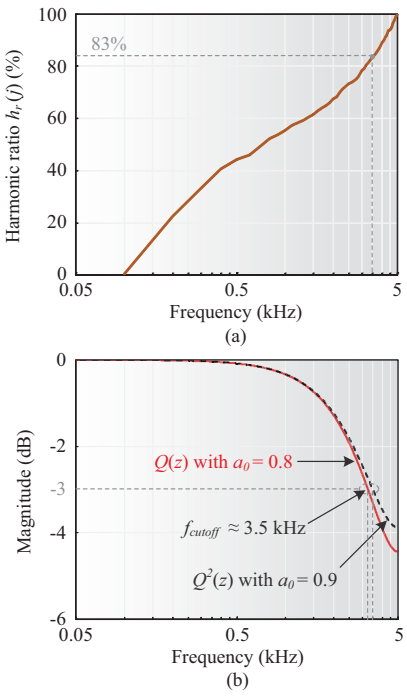

Fig. 10. Harmonic spectrum analysis under constant grid frequency $f_0 = 50$ Hz: (a) harmonic ratio $h_r(j)$ of the grid current i_g and (b) magnitude responses of the low pass filters $Q(z)$ and $Q^2(z)$.

In the case of a nominal grid frequency $f_0 = 50$ Hz, both $N = f_s/f_0 = 200$ and $p = N/4 = 50$ are integers. In those cases, the CRC, the $(4k \pm 1)$-order SHC, and the hybrid SHC control schemes are plugged into the DB controlled system to enhance the harmonic elimination. Fig. 11(a) demonstrates that the settling time of transient tracking error $e_{i_g}(t) = i_g^*(t) - i_g(t)$ with the DB and CRC control is about 0.14 sec, and Fig. 11(b) shows that the settling time of transient tracking error $e_{i_g}(t)$ with the DB and $(4k \pm 1)$-order SHC control is about 0.07 sec, and whilst the settling time of the DB with the proposed universal hybrid SHC control is about 0.08 sec as shown in Fig. 11(c). It means that the transient response of the hybrid SHC can be much faster (up to $n/2$ times) than that of the CRC. Fig. 12 shows that the steady-state responses of plugged in CRC, $(4k \pm 1)$-order SHC, and the hybrid SHC controlled single-phase system and the harmonic spectrums of the grid current i_g with THD_{i_g} = 1.4 %, THD_{i_g} = 2.35 %, and THD_{i_g} = 1.49 %, correspondingly. It is clearly indicated in Fig. 11 and Fig. 12 that both the CRC and the hybrid SHC can produce almost perfectly sinusoidal current with very low current THDs, while the $(4k \pm 1)$-order SHC control can achieve the fastest response but highest current THD among those three control schemes since it only acts on the harmonics of $(4k \pm 1)$-order. Nevertheless, the hybrid SHC control scheme with optimized control gains can be competitive to the CRC in terms of tracking accuracy, and also to the $(4k \pm 1)$-order SHC in terms of transient response. It has been verified that the hybrid SHC can offer an optimal and efficient harmonic control solution with e.g. high accuracy, fast response, and easy implementation.

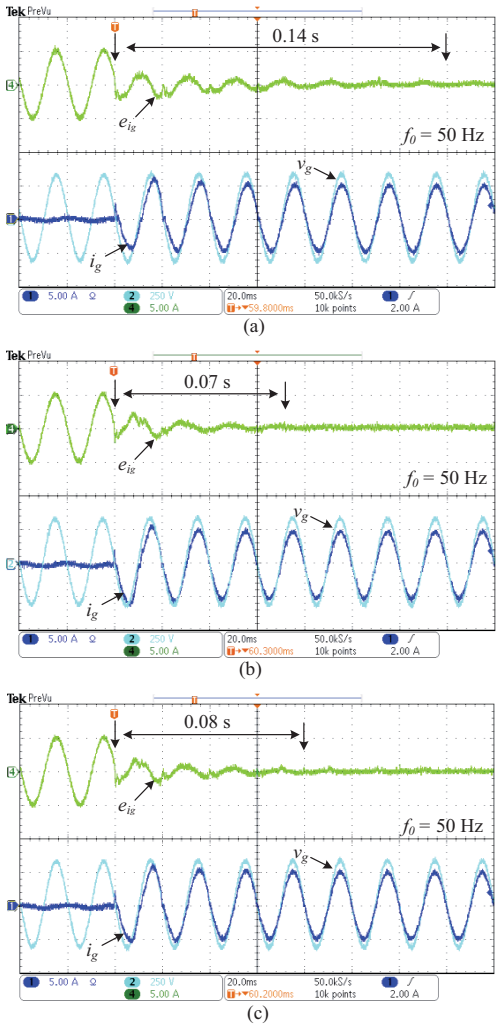

Fig. 11. Start-up transient tracking error of the grid current with different control schemes (grid voltage v_g: [250 V/div], grid current i_g: [5 A/div], tracking error e_{i_g}: [5 A/div], time: [20 ms/div]): (a) DB with the CRC control, (b) DB with the $(4k \pm 1)$-order SHC control, and (c) DB with the hybrid SHC control.

C. Experimental Results - Variable Grid Frequency

The above tests have verified the effectiveness of the CRC and the hybrid SHC schemes in terms of tracking accuracy and thus very low current THDs. However, in the case of frequency variations, e.g. if $f_0 = 50.2$ Hz, $N/4 = 49.8$ will be fractional, and if $f_0 = 49.8$ Hz, $N/4 = 50.2$ will also be fractional, the tracking accuracy of the CRC or the hybrid SHC schemes (and $4k \pm 1$ order SHC) will be significantly degraded. This has been demonstrated by Fig. 13, Fig. 14, and Table II, where the current THDs under various grid frequencies are presented. It can also be seen from Table II that the DB controller is not sensitive to frequency variations, and the $(4k \pm 1)$-order SHC has a poor tracking accuracy performance compared to the frequency adaptive CRC and the proposed FA-SHC. Moreover, without frequency adaptability for the CRC scheme, the current will be severely distorted (e.g. THD = 1.55 % if $f_0 = 50$ Hz, and THD = 6.5 % if $f_0 = 51$ Hz) as shown in Fig. 13, Fig. 14, and Table II. Besides, there will be phase shifts between the grid voltage and the grid current, leading

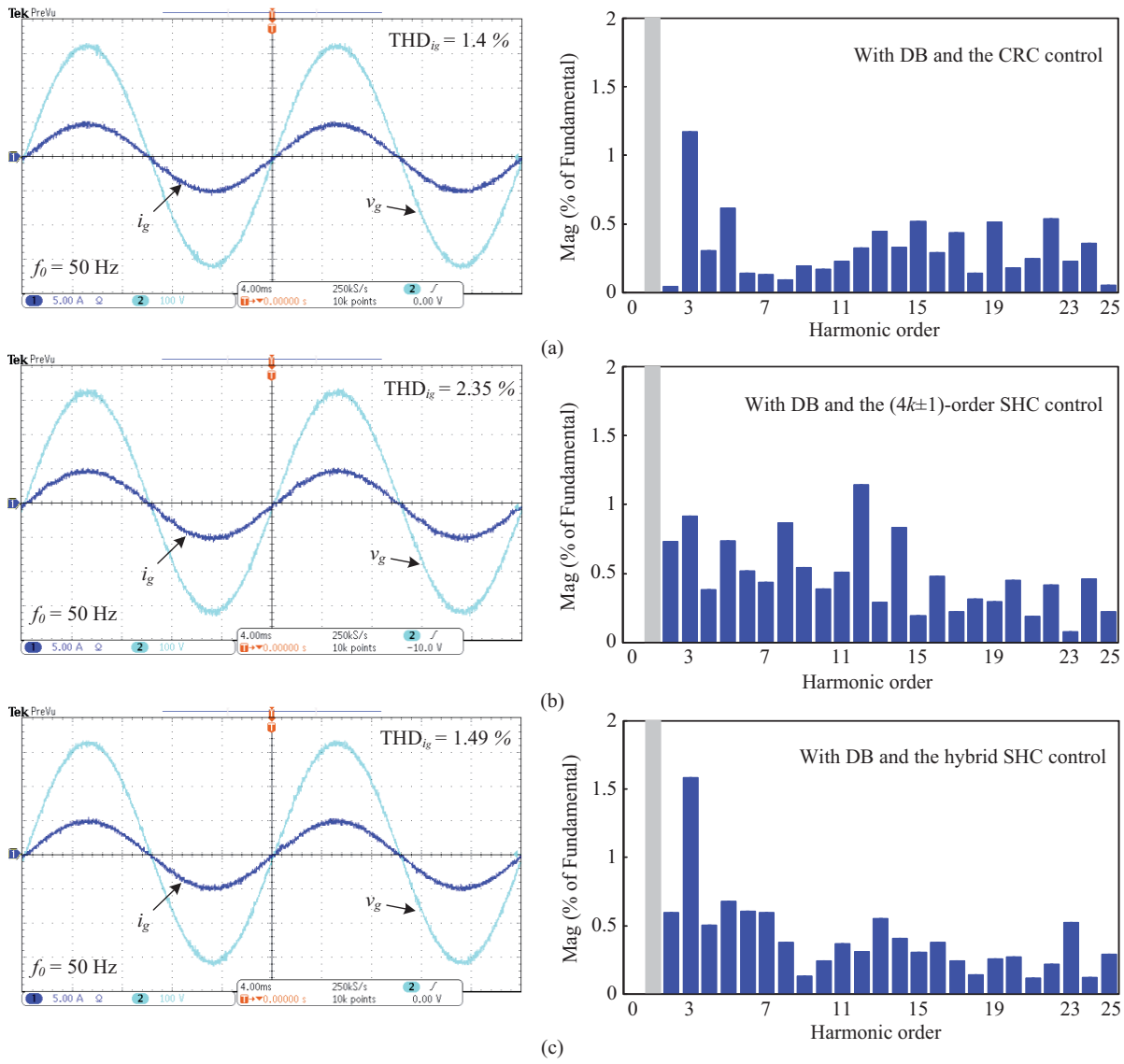

Fig. 12. Steady state performance of the single-phase grid-connected system with different control schemes in case of $f_0 = 50$ Hz (left: grid voltage v_g: [100 V/div], grid current i_g: [5 A/div], time: [4 ms/div]; right: harmonic spectrum of the grid current i_g): (a) DB with the CRC control, (b) DB with the $(4k \pm 1)$-order SHC control, and (c) DB with the hybrid SHC control.

TABLE II
CURRENT THDS UNDER VARIOUS GRID FREQUENCIES USING DIFFERENT CONTROL SCHEMES

Grid Frequency (Hz)		49	49.5	49.6	49.7	49.8	49.9	50	50.1	50.2	50.3	50.4	50.5	51
THD$_{i_g}$ (%)	DB	8.39	8.12	8.09	8.07	8.05	8.01	8	8.02	8.05	8.11	8.15	8.2	8.65
	DB+CRC	3.02	1.9	1.78	1.63	1.48	1.42	1.4	1.43	1.52	1.63	1.82	2	3.16
	DB+NA CRC	6.25	4.5	4	3.38	2.7	2	1.55	2.12	2.8	3.4	3.95	4.44	6.5
	DB+$(4k \pm 1)$ SHC	3.6	2.83	2.63	2.5	2.4	2.36	2.35	2.43	2.7	2.75	2.68	2.73	3.64
	DB+FA-SHC	3.08	2.02	1.85	1.73	1.63	1.52	1.49	1.52	1.63	1.77	1.95	2.13	3.16
Notes		NA stands for Non-Adaptive. Without specifying, the controllers are frequency adaptive.												

to a reactive power injection or absorbtion, as it is shown in Fig. 14. These are the same cases for the hybrid SHC control scheme, since it is equivalent to the CRC as discussed in § II.

In order to further evaluate the robustness and convergence rate of the proposed FA-SHC scheme and also the frequency adaptive CRC scheme in response to frequency step changes, more experiments have been carried out. Fig. 15 shows the start-up performance of the frequency adaptive CRC and the proposed FA-SHC in case of an abnormal grid frequency (i.e. $f_0 = 51$ Hz). In contrast to the start-up performance of the two controllers shown in Fig. 11, it can be seen that the frequency adaptive CRC and the proposed FA-SHC are of fast transient response regardless of the grid frequency. Additionally, the transient performance of the adaptive CRC and the proposed

TABLE III
BENCHMARKING OF THE FREQUENCY ADAPTIVE CURRENT CONTROLLERS[1]

Controller	Complexity	Approximated Delays[2]	Memory Space	Tracking Accuracy	Tracking Speed
Adaptive CRC	+	$N + N_D$	++	++	+
$(4k \pm 1)$-SHC	+	$\frac{N}{2} + N_D$	+	+	+++
FA-SHC	++	$N + N_D$	++	++	++

1. A qualitative comparison without considering $Q(z)$ and $G_f(z)$.
2. $N = \lfloor f_s/f_0 \rfloor$ with f_s being the sampling frequency and f_0 being the grid frequency. N_D has been defined in (16).

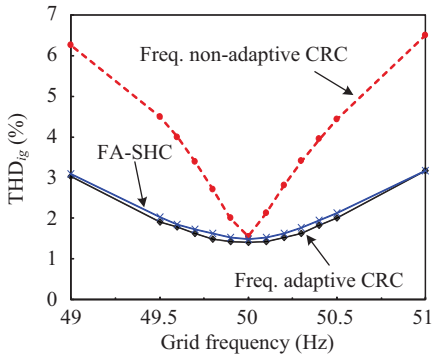

Fig. 13. Experimental comparison of frequency adaptive and frequency non-adaptive current controllers under various grid frequencies.

FA-SHC schemes under frequency step changes is presented in Fig. 16, which indicates that both the CRC and the hybrid SHC schemes with frequency adaptability are immune to grid frequency variations. As a consequence, for grid-connected applications, the proposed FA-SHC scheme is very suitable in terms of tracking accuracy, dynamic performance, and also easy for implementation. Furthermore, a benchmarking of these controllers is given in Table III, in which the more "+" means that the more complicated the controller is; the more memory space it consumes; the faster tracking it can do; or the better tracking accuracy it can achieve. It can be seen in Table III that, although the proposed FA-SHC scheme requires the most computation resources among the three controllers, it can still be implemented in a typical low-cost microcontroller, which can generate enough delays to implement those controllers [48]. Nevertheless, the proposed FA-SHC scheme will not increase too much cost in the practical applications.

V. CONCLUSIONS

An internal model principle based Frequency Adaptive Selected Harmonic Control (FA-SHC) scheme has been proposed in this paper to provide a tailor-made optimal control solution to the tracking or elimination of selective harmonic frequencies for n-pulse grid-connected inverters under normal grid frequency and also grid frequency variations. A hybrid SHC scheme has been developed firstly, and it takes advantage of the strengths of both conventional RC and multiple parallel resonant controllers in terms of high accuracy due to the removal of most of harmonics, fast transient response due to the parallel combination of optimally parameter-weighted SHC modules, cost-effective and easy real-time implementation, and

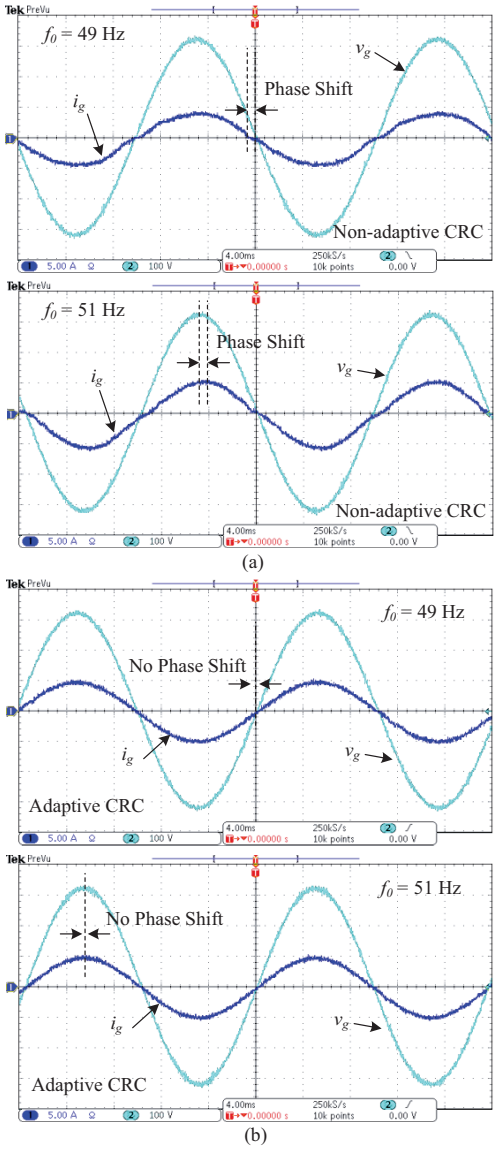

Fig. 14. Steady-state performance of frequency adaptive and frequency non-adaptive CRC current controllers under various grid frequencies (grid voltage v_g: [100 V/div] and grid current i_g: [5 A/div], time: [4 ms/div]): (a) frequency non-adaptive CRC controller and (b) frequency adaptive CRC controller.

compatible design. The analysis and synthesis of the hybrid SHC scheme have been addressed in details. The synthesis of the hybrid SHC also provides a practical framework for housing various RC schemes.

More important, the hybrid SHC has been transformed to the fractional order SHC being of frequency adaptability,

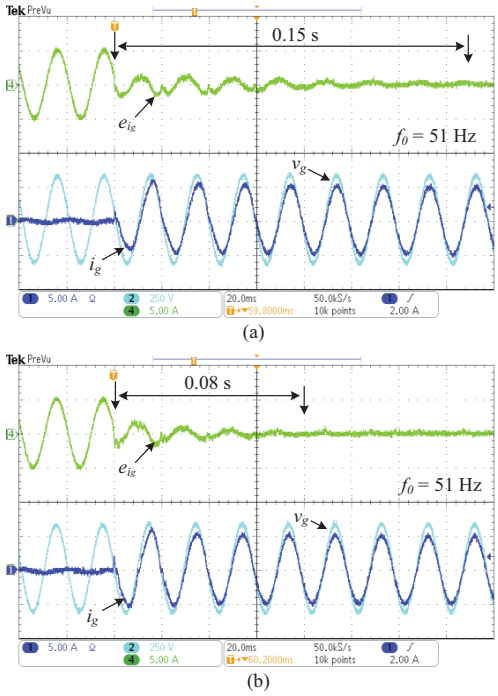

Fig. 15. Start-up transient tracking error of the grid current with different control schemes (grid voltage v_g: [250 V/div], grid current i_g: [5 A/div], tracking error e_{i_g}: [5 A/div], time: [20 ms/div]): (a) DB with the frequency adaptive CRC control and (b) DB with the FA-SHC control.

which is the proposed FA-SHC scheme. Compared to the hybrid SHC, the proposed FA-SHC requires a little more multiplications and summations to deal with the fractional order delays. As for grid-connected applications, the grid frequency is not maintained always as constant nominal value e.g. due to the generation-load imbalance and grid faults, and thus the proposed FA-SHC can be adopted to enhance the performance of grid-connected applications. A case study of a single-phase grid-connected system has been comprehensively presented in this paper. The experimental results have demonstrated and verified the effectiveness of the proposed FA-SHC scheme in terms of fast transient response, good tracking accuracy, and immunity to frequency variations.

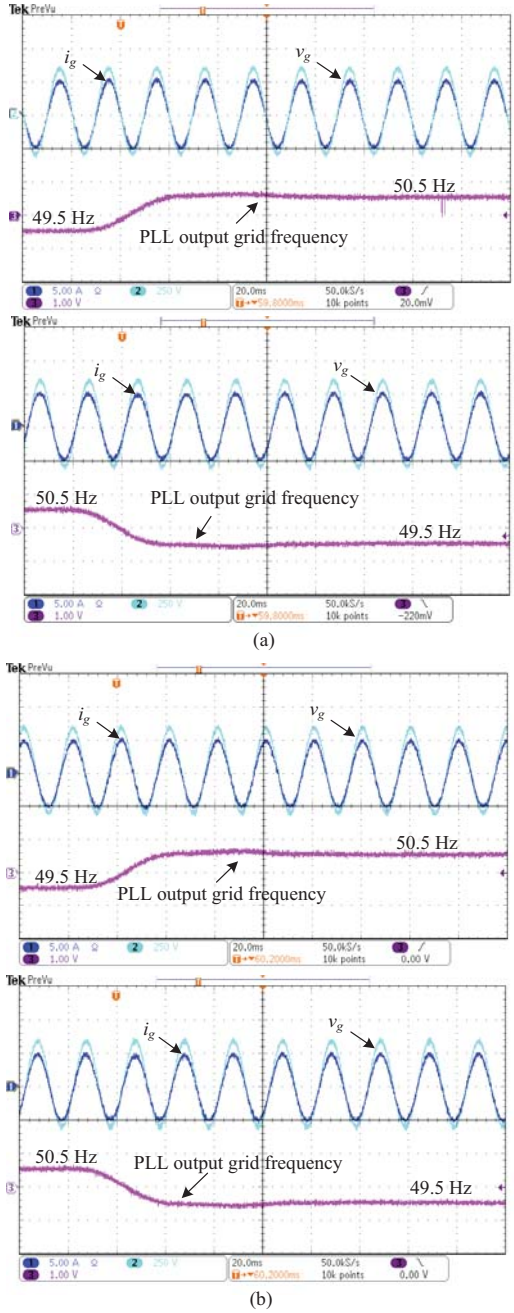

Fig. 16. Transient performance of the single-phase grid-connected system with the DB+CRC and DB+FA-SHC control schemes (grid voltage v_g: [250 V/div], grid current i_g: [5 A/div], grid frequency [1 Hz/div], time: [20 ms/div]): (a) DB with the frequency adaptive CRC control and (b) DB with the FA-SHC control (top: grid frequency 49.5 Hz $\rightarrow$ 50.5 Hz and bottom: grid frequency 50.5 Hz $\rightarrow$ 49.5 Hz).

REFERENCES

[1] F. Blaabjerg, R. Teodorescu, M. Liserre, and A.V. Timbus, "Overview of control and grid synchronization for distributed power generation systems," *IEEE Trans. Ind. Electron.*, vol. 53, no. 5, pp. 1398–1409, Oct. 2006.

[2] A.V. Timbus, M. Liserre, R. Teodorescu, P. Rodriguez, and F. Blaabjerg, "Evaluation of current controllers for distributed power generation systems," *IEEE Trans. Power Electron.*, vol. 24, no. 3, pp. 654–664, Mar. 2009.

[3] K. Zhou, Z. Qiu, N.R. Watson, and Y. Liu, "Mechanism and elimination of harmonic current injection from single-phase grid-connected PWM converters," *IET Power Electronics*, vol. 6, no. 1, pp. 88–95, Jan. 2013.

[4] Y. Yang, K. Zhou, and F. Blaabjerg, "Harmonics suppression for single-phase grid-connected PV systems in different operation modes," in *Proc. of IEEE APEC'13*, pp. 889-896, Mar. 2013.

[5] A. Kulkarni and V. John, "Mitigation of lower order harmonics in a grid-connected single-phase PV inverter," *IEEE Trans. Power Electron.*, vol. 28, no. 11, pp. 5024–5037, Nov. 2013.

[6] X. Wang, F. Blaabjerg, and W. Wu, "Modeling and analysis of harmonic stability in an AC power-electronics-based power system," *IEEE Trans. Power Electron.*, vol. PP, no. 99, pp. 1–12, early access, 2014.

[7] "IEEE Application Guide for IEEE Std 1547, IEEE Standard for Interconnecting Distributed Resources With Electric Power Systems," *IEEE Std 1547.2-2008*, 2009.

[8] S.B. Kjaer, J.K. Pedersen, and F. Blaabjerg, "A review of single-phase grid-connected inverters for photovoltaic modules," *IEEE Trans. Ind. Appl.*, vol. 41, no. 5, pp. 1292–1306, Sept./Oct. 2005.

[9] R. Teodorescu, F. Blaabjerg, M. Liserre, and P.C. Loh, "Proportional-resonant controllers and filters for grid-connected voltage-source converters," *IEE Proc. Electric Power Applications*, vol. 153, no. 5, pp. 750–762, Sept. 2006.

[10] M. Liserre, R. Teodorescu, and F. Blaabjerg, "Multiple harmonics control for three-phase grid converter systems with the use of PI-RES

current controller in a rotating frame," *IEEE Trans. Power Electron.*, vol. 21, no. 3, pp. 836–841, May 2006.
[11] R. Teodorescu, M. Liserre, and P. Rodriguez, *Grid converters for photovoltaic and wind power systems*. Hoboken, NJ, USA: Wiley, 2011.
[12] B.A. Francis and W.M. Wonham, "The internal model principle for linear multivariable regulators," *Applied mathematics and optimization*, vol. 2, no. 2, pp. 170–194, 1975.
[13] K. Zhou, W. Lu, Y. Yang, and F. Blaabjerg, "Harmonic control: A natural way to bridge resonant control and repetitive control," in *Proc. of American Control Conference (ACC)*, pp. 3189-3193, Jun. 2013.
[14] M. Tomizuka, T.-C. Tsao, and K.-K. Chew, "Analysis and synthesis of discrete-time repetitive controllers," *Journal of Dynamic Systems, Measurement, and Control*, vol. 111, no. 3, pp. 353–358, 1989.
[15] Q.-C. Zhong and T. Hornik, "Cascaded current–voltage control to improve the power quality for a grid-connected inverter with a local load," *IEEE Trans. Ind. Electron.*, vol. 60, no. 4, pp. 1344–1355, 2013.
[16] D. Chen, J. Zhang, and Z. Qian, "An improved repetitive control scheme for grid-connected inverter with frequency-adaptive capability," *IEEE Trans. Ind. Electron.*, vol. 60, no. 2, pp. 814–823, 2013.
[17] W. Lu, K. Zhou, D. Wang, and M. Cheng, "A general parallel structure repetitive control scheme for multiphase DC-AC PWM converters," *IEEE Trans. Power Electron.*, vol. 28, no. 8, pp. 3980–3987, 2013.
[18] K. Zhou, D. Wang, B. Zhang, Y. Wang, J.A. Ferreira, and S.W.H. de Haan, "Dual-mode structure digital repetitive control," *Automatica*, vol. 43, no. 3, pp. 546–554, 2007.
[19] P. Mattavelli and F.P. Marafao, "Repetitive-based control for selective harmonic compensation in active power filters," *IEEE Trans. Ind. Electron.*, vol. 51, no. 5, pp. 1018–1024, 2004.
[20] P.C. Loh, Y. Tang, F. Blaabjerg, and P. Wang, "Mixed-frame and stationary-frame repetitive control schemes for compensating typical load and grid harmonics," *IET Power Electronics*, vol. 4, no. 2, pp. 218–226, 2011.
[21] M. Ciobotaru, R. Teodorescu, and F. Blaabjerg, "Control of single-stage single-phase PV inverter," in *Proc. of EPE'05*, pp. P.1-P.10, 2005.
[22] M. Rashed, C. Klumpner, and G. Asher, "Repetitive and resonant control for a single-phase grid-connected hybrid cascaded multilevel converter," *IEEE Trans. Power Electron.*, vol. 28, no. 5, pp. 2224–2234, 2013.
[23] J.R. Wells, B.M. Nee, P.L. Chapman, and P.T. Krein, "Selective harmonic control: a general problem formulation and selected solutions," *IEEE Trans. Power Electron.*, vol. 20, no. 6, pp. 1337–1345, 2005.
[24] S.A. Dahidah and V.G. Agelidis, "Selective harmonic elimination PWM control for cascaded multilevel voltage source converters: A generalized formula," *IEEE Trans. Power Electron.*, vol. 23, no. 4, pp. 1620–1630, 2008.
[25] R. Ni, Y.W. Li, Y. Zhang, N.R. Zargari, and Z. Cheng, "Virtual impedance-based selective harmonic compensation (VI-SHC) PWM for current source rectifiers," *IEEE Trans. Power Electron.*, vol. 29, no. 7, pp. 3346–3356, Jul. 2014.
[26] N.R.N. Ama, F.O. Martinz, L. Matakas, and F. Kassab, "Phase-locked loop based on selective harmonics elimination for utility applications," *IEEE Trans. Power Electron.*, vol. 28, no. 1, pp. 144–153, Jan. 2013.
[27] G. Escobar, P.G. Hernandez-Briones, P.R. Martinez, M. Hernandez-Gomez, and R.E. Torres-Olguin, "A repetitive-based controller for the compensation of harmonic components," *IEEE Trans. Ind. Electron.*, vol. 55, no. 8, pp. 3150–3158, Aug. 2008.
[28] R. Costa-Castelló, R. Grinó, and E. Fossas, "Odd-harmonic digital repetitive control of a single-phase current active filter," *IEEE Trans. Power Electron.*, vol. 19, no. 4, pp. 1060–1068, 2004.
[29] K. Zhou, K.-S. Low, Y. Wang, F.-L. Luo, and B. Zhang, "Zero-phase odd-harmonic repetitive controller for a single-phase PWM inverter," *IEEE Trans. Power Electron.*, vol. 21, no. 1, pp. 193–201, 2006.
[30] W. Lu, K. Zhou, D. Wang, and M. Cheng, "A generic digital $nk \pm m$ -order harmonic repetitive control scheme for PWM converters," *IEEE Trans. Ind. Electron.*, vol. 61, no. 3, pp. 1516–1527, Mar. 2014.
[31] G. Escobar, P. Mattavelli, M. Hernandez-Gomez, and P.R. Martinez-Rodriguez, "Filters with linear-phase properties for repetitive feedback," *IEEE Trans. Ind. Electron.*, vol. 61, no. 1, pp. 405–413, Jan. 2014.
[32] Z. Zou, K. Zhou, Z. Wang, and M. Cheng, "Fractional-order repetitive control of programmable AC power sources," *IET Power Electronics*, vol. 7, no. 2, pp. 431–438, Feb. 2014.
[33] M.S. Tavazoei and M. Tavakoli-Kakhki, "Compensation by fractional-order phase-lead/lag compensators," *IET Control Theory Applications*, vol. 8, no. 5, pp. 319–329, Mar. 2014.
[34] Comitato Elettrotecnico Italiano, "Reference technical rules for connecting users to the active and passive LV distribution companies of electricity," *CEI 0-21*, Dec. 2011.
[35] E. Romero-Cadaval, G. Spagnuolo, L. Garcia Franquelo, C.A. Ramos-Paja, T. Suntio, and W.M. Xiao, "Grid-connected photovoltaic generation plants: Components and operation," *IEEE Ind. Electron. Mag.*, vol. 7, no. 3, pp. 6–20, 2013.
[36] F. Gonzalez-Espin, G. Garcera, I. Patrao, and E. Figueres, "An adaptive control system for three-phase photovoltaic inverters working in a polluted and variable frequency electric grid," *IEEE Trans. Power Electron.*, vol. 27, no. 10, pp. 4248–4261, Oct. 2012.
[37] M.A. Herran, J.R. Fischer, S.A. Gonzalez, M.G. Judewicz, I. Carugati, and D.O. Carrica, "Repetitive control with adaptive sampling frequency for wind power generation systems," *IEEE Journal of Emerging and Selected Topics in Power Electronics*, vol. 2, no. 1, pp. 58–69, Mar. 2014.
[38] T. Hornik and Q.-C. Zhong, "H^∞ repetitive voltage control of grid-connected inverters with a frequency adaptive mechanism," *IET Power Electron.*, vol. 3, no. 6, pp. 925–935, Mar. 2010.
[39] Y.-Y. Tzou, S.-L. Jung, and H.-C. Yeh, "Adaptive repetitive control of PWM inverters for very low THD AC-voltage regulation with unknown loads," *IEEE Trans. Power Electron.*, vol. 14, no. 5, pp. 973–981, Sep. 1999.
[40] B.P. McGrath, D.G. Holmes, and J.J.H. Galloway, "Power converter line synchronization using a discrete fourier transform (DFT) based on a variable sample rate," *IEEE Trans. Power Electron.*, vol. 20, no. 4, pp. 877–884, 2005.
[41] Y. Yang, K. Zhou, M. Cheng, and B. Zhang, "Phase compensation multiresonant control of CVCF PWM converters," *IEEE Trans. Power Electron.*, vol. 28, no. 8, pp. 3923–3930, 2013.
[42] Y. Wang, D. Wang, B. Zhang, and K. Zhou, "Fractional delay based repetitive control with application to PWM DC/AC converters," in *Proc. of IEEE Int. Conf. on Control Applications*, pp. 928–933, 2007.
[43] T. I. Laakso, V. Valimaki, M. Karjalainen, and U. K. Laine, "Splitting the unit delay [FIR/all pass filters design]," *IEEE Signal Process. Mag.*, vol. 13, no. 1, pp. 30–60, 1996.
[44] A. Charef and T. Bensouici, "Digital fractional delay implementation based on fractional order system," *IET Signal Processing*, vol. 5, no. 6, pp. 547–556, Sept. 2011.
[45] J. Miret, M. Castilla, J. Matas, J.M. Guerrero, and J.C. Vasquez, "Selective harmonic-compensation control for single-phase active power filter with high harmonic rejection," *IEEE Trans. Ind. Electron.*, vol. 56, no. 8, pp. 3117–3127, 2009.
[46] B. Zhang, K. Zhou, Y. Wang, and D. Wang, "Performance improvement of repetitive controlled PWM inverters: A phase-lead compensation solution," *International Journal of Circuit Theory and Applications*, vol. 38, no. 5, pp. 453–469, 2010.
[47] L. Malesani, P. Mattavelli, and S. Buso, "Robust dead-beat current control for PWM rectifiers and active filters," *IEEE Trans. Ind. Appl.*, vol. 35, no. 3, pp. 613–620, 1999.
[48] Atmel Corporation, "AVR 133: Long delay generation using the AVR microcontroller," Application Note, [Online]. Available: http://www.atmel.com/Images/doc1268.pdf, Jan. 2004.

Yongheng Yang (S'12) received the B.Eng. in electrical engineering and automation from Northwestern Polytechnical University, Xian, China, in 2009. During 20092011, he was enrolled in a master-doctoral program in the School of Electrical Engineering at Southeast University, Nanjing, China. During that period, he was involved in the modeling and control of single-phase grid-connected photovoltaic (PV) systems. From March to May in 2013, he was a Visiting Scholar in the Department of Electrical and Computer Engineering at Texas A&M University, College Station, TX, USA. He is currently working toward the Ph.D. degree in the Department of Energy Technology at Aalborg University, Aalborg East, Denmark.

His research interests include grid detection, synchronization, and control of single-phase photovoltaic systems in different operation modes, and reliability for next-generation PV inverters.

Keliang Zhou (M'04 - SM'08) received the B.Sc. degree from the Huazhong University of Science and Technology, Wuhan, China, the M.Eng. degree from Wuhan Transportation University (now the Wuhan University of Technology), Wuhan, and the Ph.D. degree from Nanyang Technological University, Singapore, in 1992, 1995, and 2002, respectively.

During 2003-2006, he was a Research Fellow at Nanyang Technological University in Singapore and at Delft University of Technology in the Netherlands, respectively. From 2006 to 2014, he was with Southeast University in China and with the University of Canterbury in New Zealand, respectively. As a Senior Lecturer he joined the School of Engineering at the University of Glasgow in Scotland in 2014. He has authored or coauthored about 100 technical papers and several granted patents in relevant areas. His teaching and research interests include power electronics and electric drives, renewable energy generation, control theory and applications, and microgrid technology.

Huai Wang (S'07 - M'12) received the B.Eng. degree in Electrical and Electronic Engineering from the Huazhong University of Science and Technology, Wuhan, China, in 2007, and the Ph.D. degree in Electronic Engineering from the City University of Hong Kong, Kowloon, Hong Kong, in 2012.

He has been with Aalborg University, Aalborg, Denmark, since 2012, where he is currently an Assistant Professor with the Department of Energy Technology. He is a Visiting Scientist with the ETH Zurich, Zurich, Switzerland, from August to September, 2014 and with the Massachusetts Institute of Technology (MIT), Cambridge, MA, USA, from September to November, 2013. He was with the ABB Corporate Research Center, Baden, Switzerland, in 2009. He has contributed over 20 journal papers and filed four patents. His current research interests include the reliability of DC-link and AC filter capacitors, reliability of power electronic systems, high voltage DC-DC power converters, time-domain control of converters, and passive components reduction technologies.

Dr. Wang is a recipient of the five paper awards and project awards from industry, IEEE, and the Hong Kong Institution of Engineers. He serves the Guest Associate Editor of the IEEE TRANSACTIONS ON POWER ELECTRONICS Special Issue on Robust Design and Reliability in Power Electronics, and a Session Chair of various conferences in power electronics.

Frede Blaabjerg (S'86 - M'88 - SM'97 - F'03) was with ABB-Scandia, Randers, Denmark, from 1987 to 1988. From 1988 to 1992, he was a Ph.D. Student with Aalborg University, Aalborg, Denmark. He became an Assistant Professor in 1992, an Associate Professor in 1996, and a Full Professor of power electronics and drives in 1998. His current research interests include power electronics and its applications such as in wind turbines, PV systems, reliability, harmonics and adjustable speed drives.

He has received 15 IEEE Prize Paper Awards, the IEEE Power Electronics Society Distinguished Service Award in 2009, the EPE-PEMC Council Award in 2010, the IEEE William E. Newell Power Electronics Award 2014 and the Villum Kann Rasmussen Research Award 2014. He was an Editor-in-Chief of the IEEE TRANSACTIONS ON POWER ELECTRONICS from 2006 to 2012. He has been Distinguished Lecturer for the IEEE Power Electronics Society from 2005 to 2007 and for the IEEE Industry Applications Society from 2010 to 2011.

Danwei Wang (SM'04) received his Ph.D and MSE degrees from the University of Michigan, Ann Arbor in 1989 and 1984, respectively. He received his B.E degree from the South China University of Technology, China in 1982.

He is currently a professor in the School of Electrical and Electronic Engineering, Nanyang Technological University (NTU), Singapore. He is the director of EXQUISITUS, Centre for E-City and the deputy director of the Robotics Research Centre, NTU. He has served as general chairman, technical chairman and various positions in international conferences. He has also served as an Associate Editor of Conference Editorial Board, IEEE Control Systems Society. He is an Associate Editor of *International Journal of Humanoid Robotics* and invited guest editor of various international journals. He was a recipient of Alexander von Humboldt Fellowship, Germany. He has published widely in the areas of iterative learning control, repetitive control, fault diagnosis and failure prognosis, satellite formation dynamics and control, as well as manipulator/mobile robot dynamics, path planning, and control.

Bin Zhang (S'03 - M'06 - SM'08) received the B.E. and M.E. degrees from the Nanjing University of Science and Technology, Nanjing, China, in 1993 and 1999, respectively, and the Ph.D. degree from Nanyang Technological University, Singapore, in 2007.

He is currently with the Department of Electrical Engineering, University of South Carolina, Columbia, SC, USA. Before that, he was with R&D, General Motors, Detroit, MI, USA, with Impact Technologies, Rochester, NY, USA, and with the Georgia Institute of Technology, Atlanta, GA, USA. His interests are prognostics and health management, power electronics, and intelligent systems and controls.